Combustion of Polymer Fuel-Spheres at Elevated Pressures

Takeo SAITO and Akira IWAMA

Institute of Space and Aeronautical Science, The University of Tokyo, Komaba, Meguro-ku, Tokyo 153

(Received December 7, 1973)

Two kinds of polymer spheres polyurethane (PU) and carboxyl-terminated polybutadiene (CTPB), *ca.* 3 and 5 mm, respectively, in diameter and used currently as fuel and/or binder constituents in solid and hybrid rocket propellants, were ignited electrically with a nichrome fiber in several oxidizing gases over the range 5—30 kg/cm². Their combustion phenomena were studied photographically with a 16 mm movie camera. The combustion flame was observed by means of direct photographs, both the variation of diameter with time and the location of contact surface being measured with shadow photographs. It was shown that PU spheres are entirely liquefied, involving slight swelling just after ignition, and then burn in a similar manner to that of distilled hydrocarbon droplets. CTPB spheres were found to expand remarkably after ignition. At the first stage the surrounding product gases formed a diffusion flame, their apparent diameters remaining nearly constant for a short time. At the second stage the remainder of the carbonaceous substance continued to burn, turning to surface combustion. It can be predicted that in an actual rocket combustion chamber the surface of the fuel-binder for PU propellants is wet and that of CTPB propellants is covered with carbonaceous layer during the course of steady state burning. The overall mass burning rate is proportional to a half and 0.3 power of total pressure for PU and CTPB, respectively, depending slightly on the kind of inert gas for dilution of the oxidizing atmosphere in both cases. A combustion model for CTPB is presented and compared with experimental results.

PU and CTPB are important fuel and/or binder constituents in current hybrid and solid composite propellants. Saito[1] and Varney and Strahle[2] demonstrated that the two polymers are contrary to each other in pyrolysis behavior. This study was undertaken to clarify the burning aspects of these polymers having different pyrolysis properties in various oxidizing gases at elevated pressures.

Most experiments on polymeric materials for propellants have placed emphasis on combustion in midget hybrid motors. In such cases, the flow pattern of oxidizer exerts strong influence and the regressing surface of the polymer displays singular geometrical configuration by gas dynamic effects. Structure of the combustion zone is more complicated with the oxidizer flow line crossing boundary layer, transition from laminar flow to turbulent on the half way in the free channel, two phase flow including carbonaceous substance and piece of polymer torn off,[3] and solid-liquid-gas reaction. Study of the combustion of polymer at simplified condition is therefore necessary for explaining this complexity of hybrid and composite propellant combustion phenomena.

The combustion of plastic materials is drawing attention from the standpoint of pollution control and fire prevention but only few reports have appeared on the combustion of polymers. Essenhigh,[4] who studied some thermoplastic polymers burning in quiescent atmosphere, concluded that a burning constant of the Nusselt d^2 law is smaller than that of hydrocarbon oil droplet, *viz.*, the burning rate is larger because of the much closer approach of the surrounding flame to the droplet surface. We have examined whether the higher burning rate of the polymer, compared to hydrocarbon oils, is valid at elevated pressures and to predict the role of the elastomeric fuel-binder in hybrid and composite propellant combustion.

Equipment and Experimental Method

The experiments were performed with the apparatus and optical system shown in Fig. 1. The equipment consists of a high-pressure vessel with a window, 30 mm in width and 350 mm in length, mounted vertically at each side for observation purpose, a mixing chamber for producing a variety of ambient gases and a photographic system.

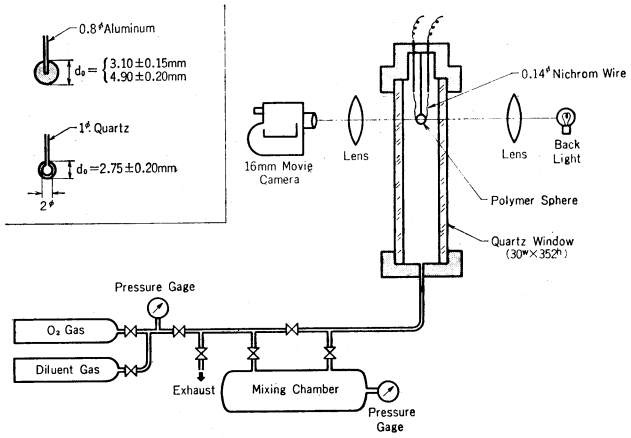

Fig. 1. Schematic diagram of the experimental apparatus.

The polymer spheres were suspended stationarily in the high-pressure vessel. PU spheres, *ca.* 3 mm in diameter, were cured at the tip of a quartz fiber; CTPB spheres, *ca.* 3 and 5 mm in diameter, were hardened and suspended at the tip of alumina fiber 0.8 mm in diameter. The spheres were ignited at the base by means of an electrically heated nichrome fiber 0.14 mm in diameter. A similar suspension method to that for CTPB was applied to PU, but the sphere could not be held stationary during the course of burning. The PU dribbled, rapidly fissuring urethane bonds and liquefying entirely to low viscosity fluid immediately after ignition. The urethane ingredient mixture was therefore cured by means of a one-shot process after being stuck to the spherical tip of a quartz fiber.

The combustion was studied with a 16 mm movie camera at the rate 49.1 frames/s. The optical system is composed of two close-up lenses and an enlargement lens set in front of a camera. Neutral density (ND) filters were used to reduce the intensity of the flame radiation on the films. While the burning spheres are shadow-photographed, the intense backward beam illuminating the sphere through the vessel is provided to drown out the surrounding flame. Variation of diameter and thickness of the boundary layers against time were measured with a film analyzer for the shadow photographs. The ambient pressure was in the range 5—30 kg/cm² (abs.). The pressurized gases, pure oxygen, oxygen diluted with nitrogen, argon and helium were used to study effects of dilution on thermal conductivity and diffusivity.

Results

Figures 2 and 3 show direct and shadow photographs of the burning PU and CTPB spheres, respectively. It is possible to distinguish two combustion phenomena for PU and CTPB. The flame of PU apparently corresponds to diffusional combustion which is similar to oil droplet combustion. On the other hand, CTPB demonstrates singularities outside the burning phenomena that were already observed on oil droplets.

Overall Mass Burning Rate. Total burning time is obtained from 16 mm movie shadow photograph records. For the *ca.* 2.7 mm diameter PU spheres in which a spherical quartz tip 2.0 mm in diameter is embraced, the total burning time t_b is obtained from the intersection of the extrapolation of variation curve of the square of diameter with the time axis. The average mass burning rate ($\dot{m}$) is calculated from initial mass of sample and total burning time.

PU: The average mass burning rate has a slight dependency upon the inert gases but an obvious dependency upon the total pressure in spite of large scattering of the data. The relation between mass burning rate and total pressure is given by $\dot{m}=\alpha P^{1/2}$ (Fig. 4). The effect of oxygen concentration in ambient gas on mass burning rate is included in factor α. Use of the diluent gases which differ in transport properties exerted a little influence on the mass burning rate, in particular He gas as a diluent indicates the tendency to increase $\dot{m}$ as compared with N_2 gas at the same oxygen concentration.

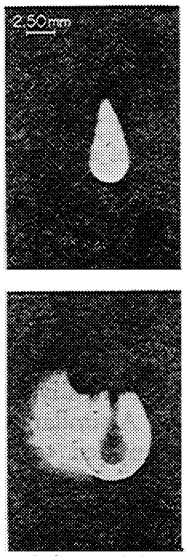

Fig. 2. Direct and shadow photographs for PU.
Upper photograph is direct one. Lower photograph is shadow one. Initial diameter: 2.65 mm. Ambient pressure: 20 kg/cm² at pure oxygen gas.

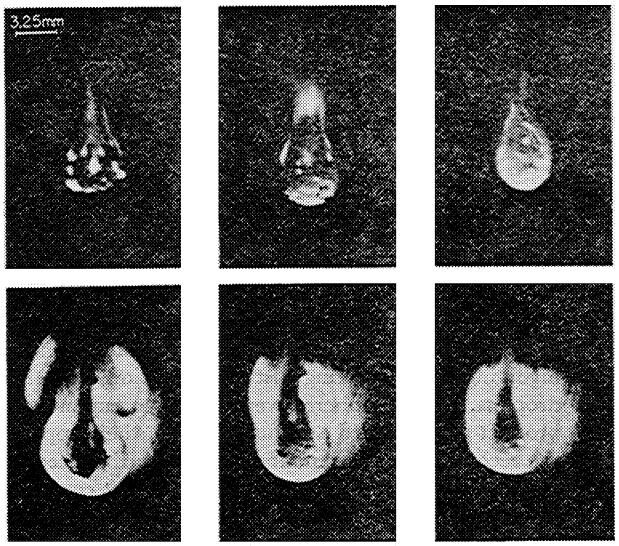

Fig. 3. Direct and shadow photographs for CTPB.
Upper photographs are direct ones. Lower photographs are shadow ones. Initial diameter: 3.25 mm. Ambient pressure: 20 kg/cm² at pure oxygen gas. Frame velocity: 49.1 frames/s.
a. 33th frame. b. 75th frame. c. 106th frame.

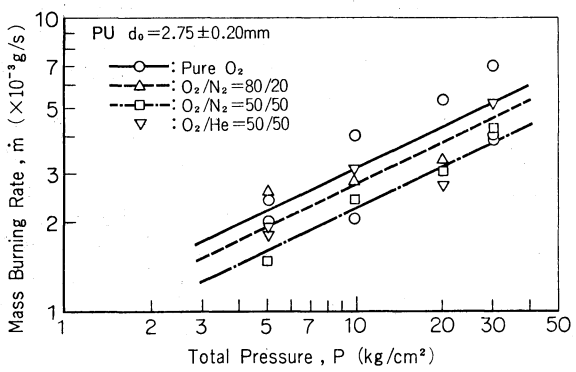

Fig. 4. Dependence of mass burning rate for PU on total pressure.

CTPB: The average mass burning rate for CTPB increases with an increase in the initial diameter of the sphere. Substitution of one diluent by another resulted in a somewhat different mass burning rate. For the sphere with initial diameter 4.9 mm, He and Ar included in oxygen gas lead to 10% higher mass burning rate than nitrogen gas dilution in the same fractions. However, such a difference due to the kind of diluent gas disappeared in the sphere of smaller initial diameter and lower oxygen fractions. This might be due to the coupling effect of thermal conductivity and diffusivity for inert gases. Figure 5 shows

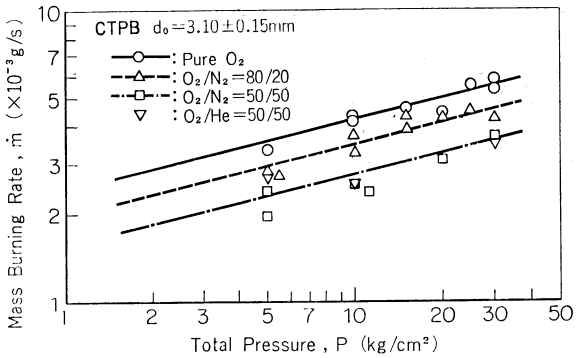

Fig. 5. Dependence of mass burning rate for CTPB on total pressure.

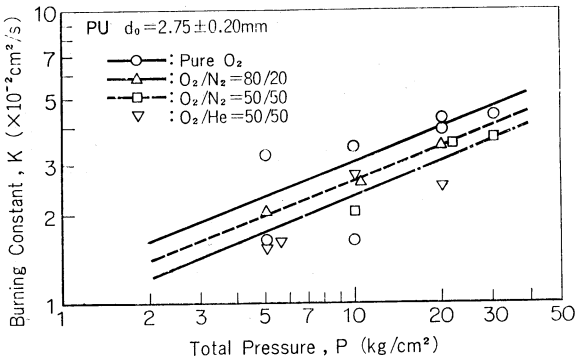

Fig. 7. Dependence of burning constant for PU on total pressure.

the dependency of the mass burning rate on total pressure given by $\dot{m}=\alpha' P^{0.3}$, where α' is a factor giving a measure of the dependency of oxygen fraction.

Square-of-Diameter Law. PU spheres swell a little just after ignition and liquefy quickly, their shape becoming ellipsoidal. According to Kobayashi's method,[5] the equivalent diameter is defined as

$$d = \sqrt[3]{a^2 b}$$

where a is a minor axis and b a major axis.

On the other hand, CTPB remains in the solid state in the core during most of the burning period and exhibits complex aspects at the surface. Closer examination revealed that the evolution of the shape of the burning drop is irregular and at lower pressures, in particular, the shape is apt to be far from spherical. The top of the drop shows a rough surface. The maximum horizontal diameter of the drop is therefore assumed to be an equivalent diameter for CTPB.

PU: After passing through a short expanding process, PU spheres decrease according to the d^2 law. Figure 6 shows plots of the variation of a PU drop diameter emerging on each frame of the 16 mm movie film. At a higher mass fraction of oxygen, discrete changes of apparent diameters exist which result from liquid-phase bubbling based on thermal cracking beneath the surface and which in turn bring about flickering at the flame front.

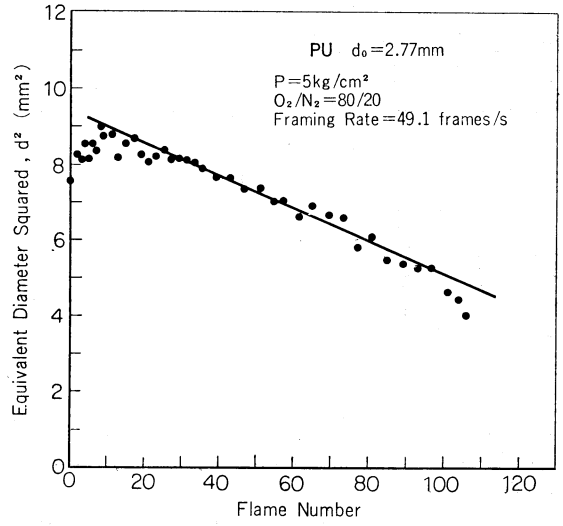

Fig. 6. Variation of equivalent diameter squared for PU with time.

The burning constant defined by $d_0^2-d^2=K(t-t_0)$ was derived by the method of least squares for diameter regressing drop during a limited period of steady state burning. In Fig. 7 the burning constant K is plotted *versus* P, the following relation being found.

$$K = \beta P^{0.4}$$

where β is a factor including dependence of oxygen fraction. Conventional oil droplets have 0.25[6] for this pressure index of the burning constant, the pressure index of PU being nearly equal to that for benzene.[7]

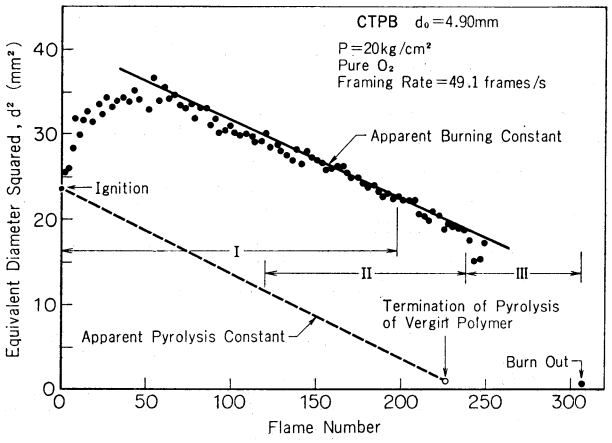

Fig. 8. Variation of equivalent diameter squared for CTPB with time.

CTPB: Figure 8 gives the change of the square of diameter during the life of a CTPB sphere in three stages:

(1) period between ignition and termination of gas emission from all burning surfaces except the top.

(2) period during surface combustion, *i.e.*, the period in which d^2 law holds. At this stage a superposition of the first stage exists.

(3) period during which the shapes change at random, the remaining cenosphere being extinguished.

At the first stage, the sphere of CTPB repeated swelling and contraction in low frequency in the order of 7—10 Hz for some time after ignition. However, the average diameter tends to be nearly constant, though for only a short time, after the initial transient period. Large scale heterogeneity of the evolving gases from surface resulted in formation of a lace pattern, producing a collection of numerous flamelets. The

porous carbonaceous substance which had become spherical was presumed to include virgin plastic. This was confirmed by interruption of burning half way, based on free falling of burning polymer spheres into a water pool.[8] From this time (second stage), the sphere began to regress along the curve of d^2 law. The coexistence of a diffusion flame formed by ambient oxygen and pyrolyzing gases with a surface combustion was observed. The linear relation between square diameter and time is valid even while virgin polymer remains, being covered with a carbonaceous layer. At the third stage, the cenosphere produced by an internal reaction occurring with the invasion of oxidizing gases into the porous layer, *i.e.*, produced by further cracking of the non-volatile carbonaceous residue, was swept out rapidly by the flame or flown away by natural convection. Apparent pyrolysis constant K_d (Fig. 8) is defined as the slope of the broken line d_0^2/t_d, linked between equivalent diameter squared at ignition d_0^2 and termination time of pyrolysis gas emission from all surfaces of burning polymer spheres. Here, the termination time of pyrolysis of virgin polymer, *i.e.*, termination of pyrolysis gas emission from all surfaces, which is defined much better than that from all surfaces except the top, was taken as t_d. Though the apparent burning constant K_r' for carbonaceous residue at the second stage, *i.e.*, the slope of the solid line, has very large scattering and even a tendency to decrease as ambient pressure increases, the corrected burning constant K_r divided by the squared swelling factor showed smaller scattering. At the third stage the shape of the porous carbonaceous residue, *i.e.*, cenosphere, changed entirely at random, and the horizontal diameter was therefore not measured. The scattering of the data prevented us from discriminating the effect of different diluent gas on the burning constant. However, it is evident that the burning constant may have weak dependency on P as shown in Fig. 9.

Extrapolation of the K–P curve at $O_2/N_2=50/50$ for PU (Fig. 7) gives *ca.* $K=0.9$ mm^2/s for one atmosphere. K is assumed to be *ca.* 0.8 mm^2/s at $O_2/N_2=20/80$ (in air). This corresponds to 50—80% less than constants

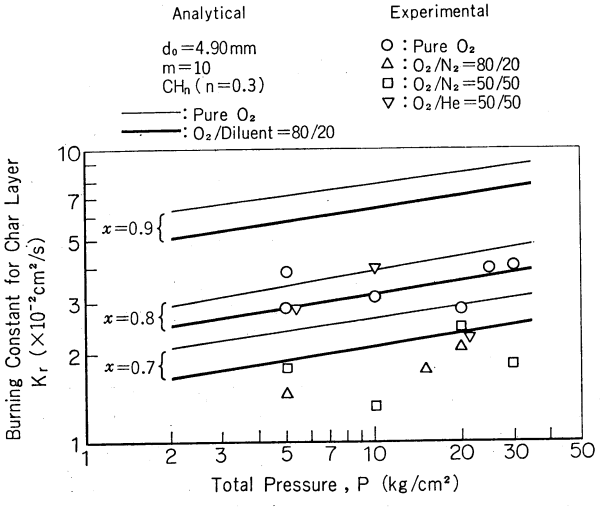

Fig. 9. Dependence of burning constant for char layer of CTPB on total pressure.

for various plastics reported by Essenhigh,[4] and suggests that PU would demonstrate substantially similar burning characteristics to those of the oil droplets.

Thickness of Contact Surface. The location of contact surface, *i.e.*, the boundary surface between surrounding ambient gas and ascending current due to natural convection, was determined by means of shadow photographs.

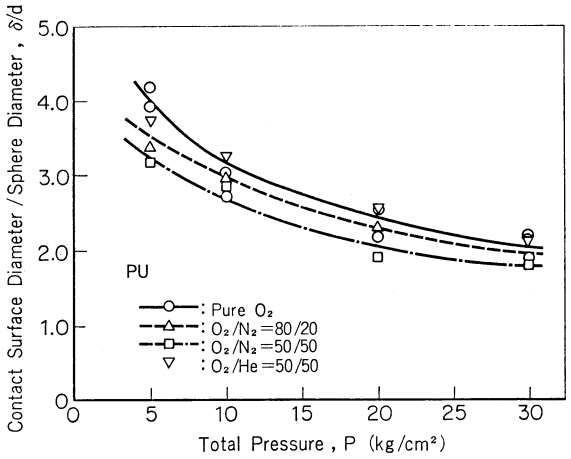

Fig. 10. δ/d for PU as a function of total pressure.

The ratio of apparent diameter of contact surface to diameter of PU sphere, δ/d, is given in Fig. 10, where δ is the maximum diameter of the contact surface envelope measured on the horizontal axis crossing at the center of the sphere. The contact surface measured in a vertical direction is five sixths of that in a horizontal direction at higher pressure and five seventhes at lower pressure. As ambient pressure decreases, δ/d increases and the contour of the contact surface expands a little in helium atmosphere because of its higher thermal conductivity.

The relationship[9] between contact surface diameter and volumetric flow rate of ascending current S is expressed by

$$\frac{\delta}{2}=\sqrt{\frac{S}{4\pi U}} \tag{1}$$

where U is the upward linear flow rate due to natural convection. Substituting $\dot{m}=\rho_g S$ into the equation and making use of the relation $\dot{m}=(\pi/4)\sigma dK$, we have

$$\frac{\delta}{d}=\sqrt{\frac{\sigma K}{8\rho_g r U}} \tag{2}$$

This equation implies that high temperature combustion of these polymers and higher density of environmental gas give a lower value of δ/d. Figure 10 shows agreement of experimental results with the trend indicated by Eq. (2). At the first stage of CTPB burning, the contact surface gives rise to oscillation in turn with the fluctuation of the burning surface. Figure 11 shows δ/d in the second stage where d^2 law holds. The contact surface becomes undulatory as oxygen fraction increases.

Swelling Factor. The swelling factor is defined as the ratio of the average maximum diameter at the first burning stage of CTPB to the initial diameter

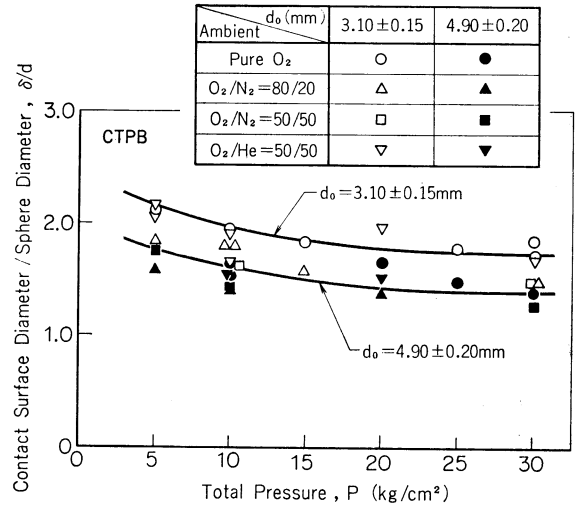

Fig. 11. δ/d for CTPB as a function of total pressure.

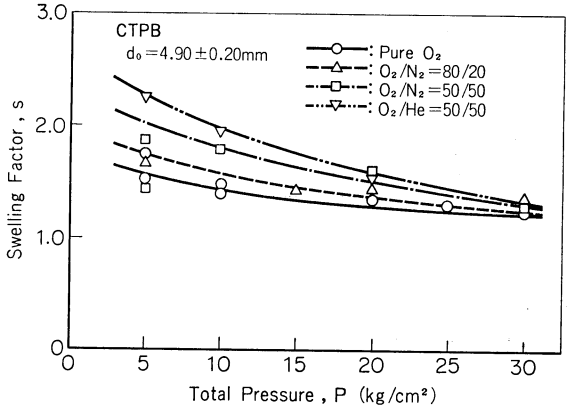

Fig. 12. Swelling factor for CTPB as a function of total pressure.

(Fig. 12). Variation of the swelling factor is affected by ambient pressure and oxygen fraction, although it is independent of the initial diameter. The use of helium gas as a diluent gave rise to an increase in the swelling factor as compared with that of N_2 diluent gas at the same oxygen fraction. Swelling for PU was negligible.

Analysis

A new combustion model for CTPB is proposed (Fig. 13). A number of semiempirical approximation apply to the region from the pyrolysis surface to the flame front:

(1) The surface of virgin polymer is maintained at constant temperature T_p with a carbonaceous layer remaining on the surface. ($\dot{m}_p=\dot{m}_g+\dot{m}_c$)

(2) The carbonaceous layer yields no dynamic interactions with the pyrolyzing gas flow (*e.g.*, its capillary flow resistance is negligible; pressure of the pyrolyzing gases passing through carbonaceous layer is constant).

(3) Quasi-steadily burning takes place.

(4) Conductive heat flux from the flame front controls the pyrolysis rate of polymer.

(5) The system is spherically symmetric.

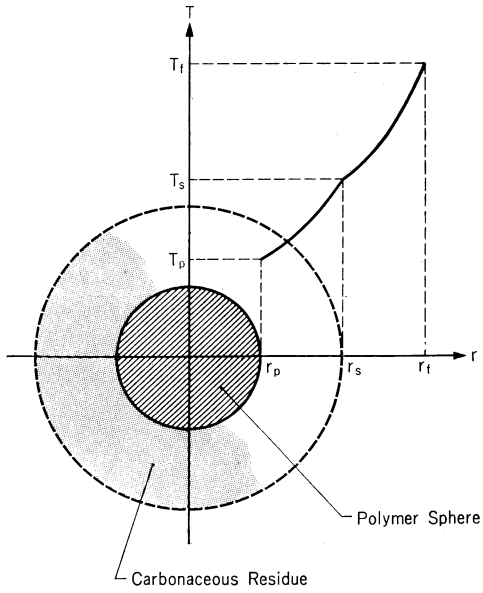

Fig. 13. A new combustion model for the sphere of CTPB.

(6) The heat released as a result of chemical reaction is removed by heat conduction and mass transport, *i.e.*, radiation and thermal convection are negligible.

(7) Temperature inclination inside virgin polymer is negligible.

The heat flow to the virgin polymer surface should balance only the heat needed for pyrolysis reaction, since the heat flow into the interior of the virgin polymer can be neglected on account of (7).

$$Q_v = h_v\dot{m}_p \doteqdot -4\pi r_p^2 q_v|_{r=r_p} \tag{3}$$

In addition, the heat flux to the virgin polymer surface is

$$q_v = -\bar{k}\frac{dT}{dr}\bigg|_{r=r_p} \tag{4}$$

where h_v is the pyrolysis heat per unit mass of polymer, $\dot{m}_p$ the mass pyrolysis rate and $\bar{k}$ the effective thermal conductivity of carbonaceous layer impregnated with pyrolyzing gases. The heat transport equation in terms of spherical coordinates would be written as

$$\rho_g c_p v_r\frac{dT}{dr} = \frac{\bar{k}}{r^2}\frac{d}{dr}\left(r^2\frac{dT}{dr}\right) \tag{5}$$

if the heat transfer between carbonaceous substance and gas flow is accomplished very quickly because of high porosity. Here, c_p is specific heat at constant pressure for gas and v_r the radial velocity. Equation (5) should be supplemented with boundary conditions:

$$T = T_s \text{ at } r = r_s$$
$$T = T_p \text{ at } r = r_p$$

The solution of Eq. (5) is given by

$$\frac{T-T_s}{T_p-T_s} = \frac{e^{-1/Ar}-e^{-1/Ar_s}}{e^{-1/Ar_p}-e^{-1/Ar_s}} \tag{6}$$

where $A=4\pi\bar{k}/c_p\dot{m}_g$ and $\dot{m}_g=4\pi r^2\rho_g v_r$. Substituting Eq. (6) into Eq. (4), we obtain

$$q_v|_{r=r_p} = -\bar{k}\frac{T_p-T_s}{Ar_p^2}\frac{e^{-1/Ar_p}}{e^{-1/Ar_p}-e^{-1/Ar_s}} \tag{7}$$

Substituting Eq. (7) into Eq. (3), we get

$$h_v\dot{m}_p = \frac{\dot{m}_g c_p(T_p - T_S)}{1-e^{-1/4(1/r_S-1/r_p)}} \tag{8}$$

The fraction of the polymer converted into gases on account of pyrolysis is defined as

$$\dot{m}_g = x\dot{m}_p, \qquad 0<x<1$$

Rewriting Eq. (8) with use of this definition, we have

$$\dot{m}_g = \frac{4\pi\bar{k}}{\left(\frac{1}{r_p}-\frac{1}{r_S}\right)c_p} \ln\left\{1+\frac{xc_p(T_S-T_p)}{h_v}\right\} \tag{9}$$

If polymer density σ is constant, the pyrolysis rate of the polymer can be expressed by

$$\dot{m}_p = -4\pi r_p^2\sigma\frac{dr_p}{dt} \tag{10}$$

Combination of Eqs. (9) and (10) gives

$$-xr_p^2\sigma\frac{dr_p}{dt} = \frac{\bar{k}}{c_p\left(\frac{1}{r_p}-\frac{1}{r_S}\right)} \ln\left\{1+\frac{xc_p(T_S-T_p)}{h_v}\right\} \tag{11}$$

On integration, we obtain

$$xr_0^2\left\{\frac{1}{2}-\frac{r_0}{3r_S}\right\} = t_d\frac{\bar{k}}{c_p\sigma} \ln\left\{1+\frac{xc_p(T_S-T_p)}{h_v}\right\} \tag{12}$$

where r_0/r_S is a factor combined with a swelling factor, s, as follows:

$$d_S^0 = d_0^2 + 0.8\{(sd_0)^2-d_0^2\} \tag{13}$$

The diameter of the carbonaceous layer is assumed to maintain a constant diameter squared which is averaged over the entire burning time at the first stage. Estimation of $\bar{k}$ in Eq. (12) is made by the equation

$$\bar{k} \approx \varepsilon k_g + (1-\varepsilon)k_s$$

where k_g and k_s are the thermal conductivity of pyrolyzing gases and carbonaceous substance, respectively, and ε the volumetric fraction of pyrolysis gases contained in char layer. We adopted the heat capacity of propane at $(T_S+T_p)/2$ for the approximation of heat capacity of the pyrolysis gases. From Eq. (12), we obtain the following relation for initial diameter:

$$d_0^2 = K_d t_d$$

where apparent pyrolysis constant K_d is:

$$K_d = \frac{4\bar{k}}{\left\{\frac{1}{2}-\frac{r_0}{3r_S}\right\}xc_p\sigma} \ln\left\{1+\frac{xc_p(T_S-T_p)}{h_v}\right\} \tag{14}$$

The equation indicates no explicit dependence of K_d on ambient pressure. It is apparent, however, that this expression becomes determinate when T_S or x is given as a function of total pressure and oxygen fraction by experiment.

The burning stage of CTPB transfers from gas-phase combustion of pyrolysis gas surrounding the surface of the carbonaceous layer to surface combustion similar to simple carbon. If the rate-determining process of regression for the carbonaceous layer is the diffusion of oxygen onto the surface, the specific reaction rate would be given by

$$R_S = -k_0(p_{ox}-p_S)$$

where k_0 is the velocity constant for mass transfer, p_{ox} the oxygen pressure in ambient gas and p_S the oxygen pressure on the surface of the carbonaceous layer. From the diffusion equation k_0 is given by

$$k_0 = \frac{DM_o}{RT_{r_c}\left(\frac{2r_c}{\delta}-1\right)} \tag{15}$$

where r_C is the carbonaceous layer radius, D the diffusivity for oxygen gas through combustion products, R the gas constant, δ the contact surface diameter and M_O the oxygen molecular weight. Since generally $p_{ox} \gg p_S$, the specific reaction constant can be given by

$$R_S = \frac{DM_o}{RT_{r_c}\left(1-\frac{2r_c}{\delta}\right)}p_{ox} \tag{16}$$

We shall now consider the stoichiometric reaction concerning the surface burning process which is given as follows.

$$CH_n + \left(1+\frac{1}{4}n\right)O_2 \longrightarrow CO_2 + \frac{n}{2}H_2O$$

On the other hand, the specific consumption rate for the carbonaceous sphere is given by

$$\frac{\dot{m}_c}{4\pi r_c^2} = -\rho_c\frac{dr_c}{dt} \tag{17}$$

From Eqs. (16) and (17), we get

$$-\frac{\rho_c}{M_c}\frac{dr_c}{dt} = \frac{1}{M_o\left(1+\frac{1}{4}n\right)}\frac{DM_o}{RT_{r_c}\left(1-\frac{2r_c}{\delta}\right)}p_{ox} \tag{18}$$

where ρ_C and M_C are apparent density for char layer and molecular weight for carbonaceous substance, respectively. We have herewith

$$\rho_c = \left(\frac{d_0}{d_S}\right)^3\sigma(1-x)$$

where d_S is as assumed in Eq. (13). Thus on integration of Eq. (18), we get

$$d_S^2-d_0^2 = \frac{8M_cDp_{ox}}{\left(1+\frac{1}{4}n\right)\rho_cRT\left(1-\frac{2r_c}{\delta}\right)}(t-t_0) \tag{19}$$

Since diffusion coefficient is proportional to ambient temperature and inverse to total pressure, apparent burning constant K_r' for carbonaceous layer is given by

$$K_r' = 8\frac{M_c}{1+\frac{1}{4}n}\frac{D^0p_{ox}}{\rho_cRT^0\left(1-\frac{d_c}{\delta}\right)}\frac{1}{P}\frac{T}{T^0} \tag{20}$$

where D^0 is diffusion coefficient at 273 K and one atmospheric pressure, the relation $T=(T_C+T_\infty)/2$ being adopted. Surface combustion temperature T_C at carbonaceous layer surface is then assumed to be proportional to total pressure; we can put $T_C=T_{C_0}P^{1/m}$. Here, T_{C_0} is the surface combustion temperature at atmospheric pressure dependent on oxygen fraction. $T_{C_0}=1500$ K is assumed for pure oxygen. The burning constant K_r, *i.e.*, K_r'/s'^2, is calculated by means of the above expression, where $s'^2=1+0.8(s^2-1)$ from Eq. (13).

Discussion

The process of combustion of CTPB sphere in a quiescent oxidizing gas is characterized by the develop-

ment of gaseous diffusion flame and subsequent surface combustion of char layer. High permeability for gases and high effective thermal conductivity of such a carbonaceous layer seem to introduce a mass burning rate about one and a quarter times as large as that of PU sphere. The comparatively greater apparent pyrolysis constant K_d for CTPB virgin polymer is also deduced to be mainly due to the thermal factor of the char layer.

The mass burning rates for PU and CTPB presumed at one atmosphere by the extrapolation method are given in Tables 1 and 2, respectively.

Table 1. Mass burning rate for PU at one atmosphere (mg/s)

Ambient	d_0=2.75± 0.20 mm
Pure O_2	1.1
O_2/N_2=80/20	0.9
O_2/N_2=50/50	0.75

Table 2. Mass burning rate for CTPB at one atmosphere (mg/s)

Ambient	d_0	
	4.90±0.20 mm	3.10±0.15 mm
Pure O_2	4.4	2.4
O_2/N_2=80/20	3.1	2.0
O_2/N_2=50/50	2.5	1.5

The first two stages are mostly the time denoted by t_d required for the burning of gases emitted from virgin polymer and a latter part of the second and the third stages are the time (t_S) of surface combustion including internal oxidation reaction. The partial superposition of the process of gas phase and surface combustion becomes considerably greater as the ambient pressure increases. For instance, t_d/t_b equals 0.75 and occurrence

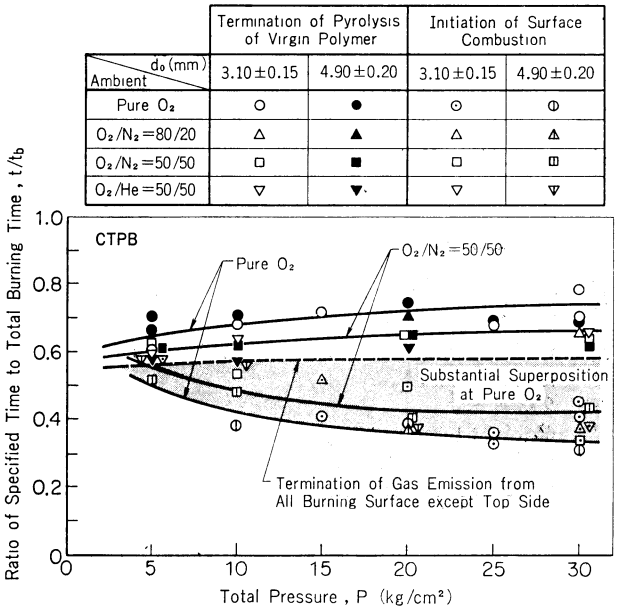

Fig. 14. Variation of ratio of specified time to total burning time with total pressure for CTPB.

of the incipient surface combustion is observed when 35% of the total time of combustion has elapsed at 30 kg/cm² of pure O_2. This is shown in Fig. 14, where the broken line denotes the time when the emission of pyrolysis gases terminates from all burning surfaces except the top at the base of a supporting fiber. However, plotting for each emission is ommitted in order to avoid complexity of the figure. In this case the time of substantial superposition of both processes is approximately 20% of the total time of combustion. Afterwards, pyrolyzing gases are emitted only from the top of the sphere. At lower pressures such as 5 kg/cm² the total time of combustion can be written as

$$t_d + t_S = t_b$$

The region of gas-phase diffusional combustion, in turn, can be divided into a process in which vigorous emission of pyrolysis gases and periodically repeated swelling and contraction of sphere are observed and a process of d^2 law combustion in which a number of flamelets are established and a part of oxygen passing through undulatory flame front contributes to the process of the surface combustion. The value of t_d/t_b photographically obtained is sensitive not to the total pressure but to oxygen fraction under high pressure. However, the ratio of surface burning to the total burning time is a little stronger function of total pressure at the lower pressure below 10 kg/cm². At more elevated pressure, CTPB burning characteristics are substantially controlled by the physical nature of the carbonaceous layer.

The results are compared with analytical calculations for the CTPB combustion model for the case in which T_S is assumed to be a function of the total pressure of ambient gas for the gas-phase combustion at the first stage:

$$T_S = T_{S_0} P^{1/m'}$$

where T_{S_0} is the surface temperature of char layer during the first stage burning at one atmospheric pressure which is dependent upon oxygen fraction. T_{S_0} for pure oxygen gas as ambient gas is assumed to be 1000 K. According to the T_S—P diagram, a reasonable value for m' is 8—12. If the fraction of CTPB polymer converted into gases on account of pyrolysis reaction is presumed to be 0.7—0.9, the calculated results would be in good agreement with experimental data (Fig. 15). The parameters used in this calculation are m'=10, $\bar{k}$=0.001 cal/cm·s·deg. Similarly, the value x derived from the combustion constant for carbonaceous residue in Fig. 9 also is 0.7—0.8. In order to examine the validity of x, deduced from this analysis, a rough estimation of the apparent density of the carbonaceous layer was made by the interruption of burning at half way, yielding 0.11—0.32. The prediction based on the analytical results of the burning constant K_r for char layer of CTPB at one atmosphere including 20% oxygen by volume yielded K_r=1 mm²/s, which is nearly twice as large as the data of some plastics forming a carbonaceous layer at the second burning stage defined here such as cellulose acetate, phenolic resin and polycarbonate.[4]

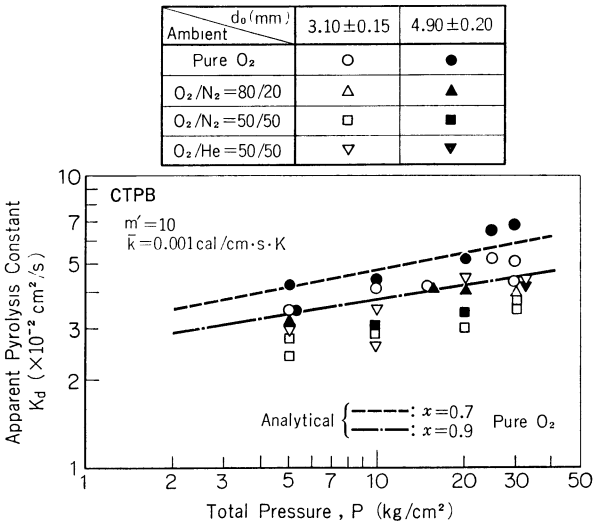

Fig. 15. Comparison of analytical results with experimental data for apparent pyrolysis constant for virgin polymer of CTPB.

Our emphasis on the CTPB burning aspects introduced by the existence of a freely-gas-permeable carbonaceous layer is to a certain extent justified by these experimental observations differing from the PU sphere burning such as common hydrocarbon droplets.

Conclusion

(1) The burning surface of PU spheres is always covered with a liquefied layer, while that of CTPB spheres remains a highly porous char layer under steady state combustion.

(2) The pressure index of the overall mass burning rates for PU and CTPB spheres are 0.5 and 0.3, respectively. Dependence of the burning constants upon the total pressure is given as follows:

$K=\beta P^{0.4}$ for PU. (experimental)

$K_d=\gamma P^{1/6}$ for virgin polymer of CTPB. (analytical)

$K_r=\gamma' P^{1/6}$ for char layer of CTPB. (analytical)

PU spheres which burn in a similar mechanism to that oil droplets regress with a rate having pressure index close to that of the burning constant for oil droplets.

(3) 70—90% of CTPB by weight is emitted as pyrolysis gases from virgin polymer on account of pyrolysis reaction and consumed in a gaseous diffusion flame with oxidizing gases, and the remainder proceeds to burn subsequently in a surface combustion mechanism.

(4) Analytical results based on a new combustion model for CTPB, which has a char layer structure formed by pyrolysis reaction, agreed with experimental observations, particularly in connection with the life of virgin polymer spheres and the fraction of the char layer.

Nomenclature

a minor axis for ellipsoid, cm
A $4\pi\bar{k}/c_p\dot{m}_g$, 1/cm
b major axis for ellipsoid, cm
c_p specific heat at constant pressure for pyrolysis gas, cal/g·K
d diameter, cm
d_0 initial diameter, cm
d_c diameter for char layer at surface combustion period, cm
d_S diameter for char layer assumed constant during gas-phase combustion, cm
D diffusion coefficient, cm²/s
D^0 diffusion coefficient at 273 K and one atmospheric pressure, cm²/s
h_v pyrolysis heat per unit mass, cal/g
$\bar{k}$ effective thermal conductivity for char layer impregnated with pyrolysis gas, cal/s·cm·K
k_0 velocity constant for mass transfer, g/s·cm²·atm
k_g thermal conductivity for pyrolysis gas, cal/s·cm·K
k_s thermal conductivity for carbonaceous substance, cal/s·cm·K
K burning constant, cm²/s
K_d apparent pyrolysis constant for virgin polymer of CTPB, cm²/s
K_r (corrected) burning constant for char layer of CTPB, cm²/s
K'_r apparent burning constant for char layer of CTPB, cm²/s
m reciprocal of pressure index
m' reciprocal of pressure index
$\dot{m}$ average mass burning rate, g/s
$\dot{m}_c$ formation rate for carbonaceous substance, g/s
$\dot{m}_g$ evolution rate for pyrolysis gas, g/s
$\dot{m}_p$ pyrolysis rate for polymer, g/s
M_c molecular weight for carbonaceous substance, g/mol
M_o oxygen molecular weight, g/mol
p_{ox} oxygen pressure in ambient gas, kg/cm²
p_S oxygen pressure on the surface of char layer, kg/cm²
P total pressure, kg/cm²
q_v heat flux, cal/s·cm²
Q_v total rate of heat flow to virgin polymer sphere, cal/s
r radius, cm
r_0 initial radius, cm
r_c radius for char layer at surface combustion period, cm
r_p radius for virgin polymer sphere, cm
r_S radius for char layer assumed constant during gas-phase combustion, cm
R gas constant, cm³·atm/K·mol
R_S specific reaction rate, g/cm²·s
s swelling factor
s'^2 $1+0.8(s^2-1)$ from Eq. (13)
S volumetric flow rate for ascending current, cm/s
t time, s
t_0 initial time, s
t_b total burning time, s
t_d termination time of pyrolysis gas emission from all burning surfaces, s
t_S surface combustion time for char layer, s
T temperature, K
T^0 273 K
T_∞ ambient temperature, K
T_C surface combustion temperature for char layer, K
T_{C_0} surface combustion temperature for char layer at one atmospheric pressure, K
T_p surface temperature for virgin polymer, K
T_S surface temperature for char layer during gas-phase combustion, K
T_{S_0} surface temperature for char layer during gas-phase combustion at one atmospheric pressure, K

U rate for natural convection, cm/s
v_r radial velocity for pyrolysis gas, cm/s
x fraction of polymer converted into gas
α factor involving the effect of oxygen fraction in mass burning rate for PU
α' factor involving the effect of oxygen fraction on mass burning rate for CTPB
β factor involving the effect of oxygen fraction on burning constant for PU
γ factor involving the effect of oxygen fraction on apparent pyrolysis constant for CTPB
γ' factor involving the effect of oxygen fraction on burning constant for CTPB
δ contact surface diameter, cm
ε volumetric fraction of pyrolysis gas contained in char layer
ρ_c apparent density for char layer, g/cm^3
ρ_g density for pyrolysis gas, g/cm^3
σ density for polymer, g/cm^3

References

1) T. Saito, Thesis, the University of Tokyo (1974).
2) A. M. Varney and W. C. Strahle, *Comb. Flame*, **16**, 1 (1967).
3) L. Nadaud and J. Biasini, *Rech. Aer.*, No. 117, 3 (1967).
4) R. H. Essenhigh, *Fuel*, **48**, 330 (1969).
5) K. Kobayashi, "5th Symposium (International) on Combustion," Reinhold, New York (1955), p. 141.
6) A. R. Hall and J. Diederichsen, "4th Symposium (International) on Combustion," Williams and Wilkins Co., Baltimore (1954), p. 837.
7) M. Goldsmith, *Jet Propulsion*, **26**, 172 (1956).
8) T. Saito and A. Iwama, *Chem. Lett.*, **1974**, 389.
9) W. A. Rosser, *Comb. Flame*, **11**, 442 (1967).